Modeling a corrugating-medium paper machine for improved edgewise compressive strength

Gary L. Jones

ABSTRACT: Using a modular analysis of pulp and paper systems simulation allows development of a detailed model of a corrugating paper machine. The model predicts tensile strength and compressive properties with variations in papermaking conditions such as old-corrugated-clippings content, refiner load, press load, machine speed, and calender load. Statistical comparisons using machine paper and handsheet data from a three-day mill trial validated the model system.

KEYWORDS: Compression strength, converting machines, corrugating machines, corrugating medium, corrugation, edge crush resistance, mechanical properties, models, packaging papers, paper board grades, paper conversion, paper converters, paper stock, simulation, tensile properties, tensile strength.

Integrating a novel system of performance attribute (PAT) models with mass and energy balance models in a modular analysis of pulp and paper systems (MAPPS) predicts both handsheet and machine paper properties. The technique is useful for a range of grades formed with a variety of pulps.

The concept of end-use performance modelling uses nonconservative variables or PAT models. These include many of the basic properties of fibers and of the fiber network. The PAT modeling system quantifies interactions that fibers have with the fiber network, processing conditions, and end-use performance characteristics. The system offers a new approach to solve problems concerning product quality.

The PAT model used here contained a set of 29 variables to describe the state of the fiber furnish or the fiber network at each point in the papermaking process. Fiber species and suspended solids databases provided the initial PAT values. PAT models will predict property changes based on variations in pulping or papermaking operations. Paper property models based on local PAT models will predict handsheet or machine paper properties. Therefore, with this technique it is possible to determine product quality using conditions that exist from the woodyard to the reel.

PAT models have either component or network attributes. Component attributes relate to the fiber or filler and include composition, shape, surface area, other physical properties, and optical properties. Network attributes comprise contact area, bond area, and anisotropy. Anisotropy includes factors such as sidedness, formation, fiber orientation, and stress distribution. Each pulp and paper unit operation may affect each of these variables.

Previous studies showed that model predictions were reasonable and consistent for newsprint and mechanical pulping operations (*1–4*). These studies, however, did not consider variability, trends, and process sensitivity. Therefore, we designed a trial on a corrugating-medium paper machine to consider these issues and to validate the PAT system for corrugating medium. The experiment also allowed determination of the sensitivity of tensile strength and compressive properties to important independent variables such as old corrugated clippings (OCC) content, refining load, press load, and calender load.

Jones is an associate professor at the Institute of Paper Science and Technology, P. O. Box 93366, Atlanta, GA 30318.

I. Test variables and data ranges

Variable	Range	Average	Base case
OCC content, %	18–38	27	18
Primary refiner power, MJ/kg	0.104–0.366	0.204	0.104
Calender loading	on or off	-	
Tickler refiner power, MJ/kg x 1000	3.34–20.1	10.0	3.34
Wire speed, m/s	7.112 and 9.65	-	7.112
Third nip pressure, kN/m^2	84.1–113.8	100.9	84.1

II. Furnish characteristics

Attributes	Semi-chemical	Hard-wood	Soft-wood	Mixture
Average fiber length, mm	1.4	1.4	3.0	2.2
Average fiber width, mm	0.02	0.02	0.04	0.03
Yield, %	74	74	60	67
CSF, mL	656	150	667	316

Property model validation

Validation means "reasonable" agreement between measurements and predictions. In our case it also considers measurement error and other sources of variation such as cross-direction (CD) differences. The validation in this work only concerned the paper machine area. This began at the high-density tanks and included the major paper machine operations such as stock preparation, sheet forming, white water recovery, wet pressing, drying, and converting. Although CD variations normally will affect some properties, our model only considers predictions for a machine-direction (MD) profile.

Validation criteria use statistical measures of "goodness of fit" and estimates of factors contributing to variability to provide predictions. These factors are measurement error, errors in estimating process conditions, and transient effects. Predictions falling within the confidence band around mean measurements indicate a valid model. The band includes the average measurement error plus CD variability, as well as errors associated with uncertainty in input data.

Process variables

We compared measurements to predictions by examining handsheet and machine paper properties. We prepared handsheets from composite pulps collected at five locations in the paper machine area. **Table I** summarizes the primary test variables.

One important uncontrolled variable was the semichemical high-density CSF.

The original intent was to change each variable separately and to achieve a "steady state" between each change. In practice, however, several controlled and uncontrolled variables changed simultaneously. The results, therefore, show the effect of more than one variable.

Process model

There are a number of novel aspects in our corrugating-medium process model. Stream initiation blocks represent the high-density storage tanks. These blocks initialize both the material and energy attributes as well as the performance attributes of the virgin semichemical and OCC furnishes.

Because the OCC furnish is a mixture of hardwood and softwood components, we used two blocks. One represented the softwood component and the other the hardwood component. We assumed the softwood component was similar to a southern pine. We also assumed that the characteristics of the hardwood component of the OCC furnish were similar to the semichemical hardwood.

Mixing the hardwood and softwood streams provided the attributes of the OCC blend. **Table II** summarizes the attributes of these and the semichemical furnish.

We initialized the fiber tensile strengths to 10 km, the fiber modulus to 4.5 GPa, the cell wall thickness to 1.2 µm, and the specific bond strength to 0.2×10^7 Pa.

Refining of the semichemical furnish reduced its fiber length, tensile strength, and elastic modulus slightly. The refining also reduced the CSF by 15–30 mL.

The tickler refiner processed the combined OCC and semichemical fiber lines. Increased load and consistency in the tickler refiner reduced freeness and average fiber length but had little effect on other attributes.

We modelled the screening and cleaning system in detail. There was, however, very little net effect on any of the fiber attributes such as fiber length and freeness. Fiber losses from the cleaning system totaled less than 1% of total flows.

Fourdrinier blocks simulated the headbox and forming wire. These led to the determination of profiles of the drainage rate, white water consistency, mat basis weight, and mat moisture. The important factors in the forming section that influenced dry sheet properties were fiber contact area, sidedness, formation, fiber orientation, final freeness, and fiber length distribution. The formed sheet freeness and fiber length were similar to that of the tickler discharge. The lower headbox freeness was mainly a reflection of white water closure and recycling. The lower headbox freeness had little influence on final sheet properties. Headbox freeness did, however, influence machine drainage, dry line location, moisture profiles in the press section, and the steam consumption needed to achieve a final 93% dryness.

Fiber length, forming consistency, and jet-to-wire velocity ratio influenced formation levels. However, the relatively high basis weight of the corrugating medium reduced the influence of these variations. Formation variations were most important in the handsheets.

Variations in the velocity ratio of the jet to the wire had only a small effect on fiber orientation.

The fiber orientation factor is the cotangent of the average fiber orientation angle relative to the machine direction. We adjusted this initially to 1.5 and maintained it at that value during the test.

The accurate prediction of the MD-to-CD tensile strength and modulus ratios of the paper machine throughout the test confirmed our observations. The insensitivity of the tensile strength ratio to the trial variables provided further confirmation.

Press loading influenced water removal and moisture profiles in the press section as well as the steam consumption necessary to reach a fixed 93% sheet dryness. Higher press loading increased the fiber contact area to yield increased density and sheet strength.

The can dryer section determined the steam consumption required to achieve a targeted final dryness. Hydrogen bonding is an important consideration in this area. We assumed that all MD stretch due to speed differentials along the length of the machine occurred in the dryer section. We adjusted the net MD wet stretch to 2% and did not change it during the trial.

III. Measures of model validity for machine paper properties using 114 data sets

Property	*Mean*	*CV*	*Correlation coefficient*	*Confidence band, %*
MD tensile strength, km	6.0	5.98	0.994	13
CD tensile strength, km	2.54	7.43	1.01	15
MD stretch, %	1.64	5.93	0.915	27
MD/CD modulus ratio	2.36	7.18	0.995	-
MD/CD tensile strength ratio	2.35	4.78	0.998	-
Burst index	2.90	7.22	0.957	16
MD modulus, GPa	1.85	8.60	0.871	12
Caliper, mm	0.2113	5.0	1.031	-
Concora test, N	238.5	5.06	0.92	13.2
CD ring crush	0.95	18.4	1.45	39.4
CD STFI,kN/m	2.54	4.59	1.173	44
Gurley porosity	20.48	20.6	0.974	-

IV. Handsheet data using 120 data sets

Property	*Mean*	*CV*	*Correlation coefficient*	*Confidence band,%*	R^2
CSF, mL	503	12.8	1.07	-	0.984
Tensile strength, km	3.64	20.9	0.936	12	0.959
Concora test, N	242.5	19.4	0.766	13	0.964
CD ring crush	1.56	25.1	1.62	12	0.939
Burst index	2.30	18.1	1.01	20	0.968
Gurley porosity	16.0	75.2	1.03	38	0.647
Density, g/cm³	0.41	9.1	0.98	-	0.992

A calender block simulated a single-nip calender. This block densifies the sheet and changes the roughness, smoothness, gloss, and porosity of the surface. The change in density from the calender increased fiber contact but did not strongly influence bonding. Tensile strength, specific modulus, or compressive strength therefore did not change. Density and elastic modulus did change.

Property models

Paper property models provide the easiest interpretation of the effects of papermaking variables.

The Concora test is a stiffness test measured in N for corrugated board components which is indicative of box compressive strength. It is a function of flat crush as shown in Eq. 1:

$$\text{Concora test} = 235.85 + 9.09(FC - 206.7) \quad (1)$$

where

FC = flat crush, kPa.

Flat crush relates to MD short span compression length [Swedish Forest Products Research Laboratory (STFI)] by Eq. 2:

$$FC = 206.7 + 11.5(STFI_{MD} - 2.98) \quad (2)$$

where

$STFI_{MD}$ = STFI in MD, kN/m.

MD and CD STFI and ring crush relate to sheet thickness and directional elastic moduli as indicated in Eqs. 3–9:

1. Machine paper caliper

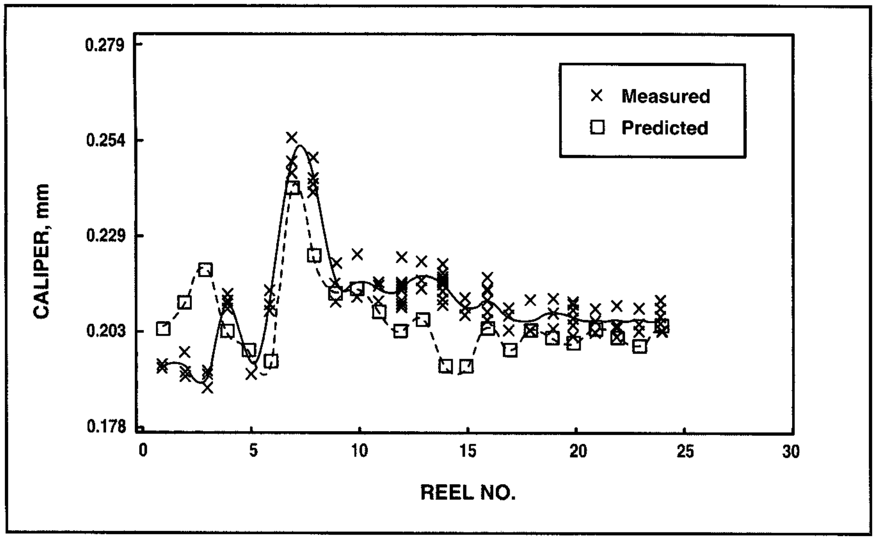

$$RC_{MD} = 0.00435T_1 + 0.00181T_2 - 0.6307 \quad (3)$$

$$RC_{CD} = 0.00435T_2 + 0.00181T_3 - 0.6307 \quad (4)$$

$$STFI_{MD} = 1.397 + 0.00613T_3 \quad (5)$$

$$STFI_{CD} = 0.800 + 0.00613T_2 \quad (6)$$

$$T_1 = (E_x t)^{3/4}(E_y t)^{1/4} \quad (7)$$

$$T_2 = (E_y t)^{3/4}(E_z t)^{1/4} \quad (8)$$

$$T_3 = (E_x t)^{3/4}(E_z t)^{1/4} \quad (9)$$

where

RC_{MD} = ring crush in MD, Kn/m

RC_{CD} = ring crush in CD, Kn/m

$STFI_{CD}$ = STFI in CD, kN/m

E_x = elastic modulus in MD, GPa

E_y = elastic modulus in CD, GPa

E_z = elastic modulus in z direction, GPa

t = sheet thickness, mm

The elastic moduli relate to fiber modulus, sheet density, bond density, bond density interaction with wet strain, and fiber orientation. Equations 10–12 provide these relationships:

$$E_x = \bar{E}_f(0.278 + \rho_b^e (7.043\rho_b^e + 6.513\theta + 1.9WS) \quad (10)$$

$$E_y = \bar{E}_f(-0.8081 + \rho_b^e (16.8 - 4.6\theta - 0.539WS)) \quad (11)$$

$$E_z = \bar{E}_f(0.308 + \rho_b^e C) \quad (12)$$

where

$$C = -1.25 + 1.44\rho_b^e + 0.011\theta + 0.029WS \quad (13)$$

where

Θ = cotangent fiber orientation angle relative to MD

WS = % MD stretch.

Equation 14 shows the relationship for the specific elastic constant. This is the dimensional elastic constant divided by bulk density. The constant is therefore independent of density and depends only on bonding, fiber modules, and residual strains in the sheet. Wet stretch and fiber orientation account for these residual strains.

$$\bar{E}_f = \frac{E_f \rho}{10\rho_b^e} \quad (14)$$

where

E_f = fiber modulus, GPa

ρ = sheet bulk density, g/cm³.

The sheet bulk density and the effective bond density are both functions of the performance attributes of the fibers and the network. These attributes include the fiber contact area, bond area, cell wall thickness, fiber stiffness, yield, freeness, and formation level. Equations 15–17 provide these relationships:

$$1/\rho = (1/\rho_u) + [(1/\rho_l) - (1/\rho_u)](1/S_b)^2 \quad (15)$$

$$1/\rho_u = 0.764 + 0.00477CSF + 0.1146CWT(S) \quad (16)$$

$$1/\rho_l = (1/\rho_u) + 43.14 + 0.08726Y - 0.5866CSF \quad (17)$$

where

ρ_u = unbonded density, g/cm³

ρ_l = upper limit to sheet density, g/cm³

CWT = cell wall thickness, µm

S = fiber stiffness factor

Y = pulping yield, %

S_b = fiber contact area.

The term S_b is the fiber contact area defined later in Eq. 20. The bond density has the same relationship as the sheet density except the bond area function, S_a, substitutes for the fiber contact function, S_b. The effective bond density is a function of bond density, formation factor, and the total fraction of suspended solids in the sheet, as seen in Eq. 18:

$$\rho_b^e = \rho_b F(1 - X_s) \quad (18)$$

where

ρ_b = bond density

F = formation factor (fraction)

X_s = fraction of suspended solids in the sheet.

The bond area function and the fiber contact function relate to the current moisture level in the sheet given by Eq. 19:

$$S_a = S_b e^{-(X_m - 0.075)} \quad (19)$$

where

X_m = weight fraction moisture in the pulp or sheet.

The term X_m is a function of dryer conditions. The fiber contact function varies throughout the thickness of the sheet. It is necessary to track the fiber contact area specifically on the top and bottom surfaces of the sheet to simulate sidedness effects through forming, pressing, and calendering. These effects include differences in smoothness, gloss, and opacity.

The fiber contact area depends on the hydrodynamic specific surface of the fibers, i.e., CSF. It is the conformability of the fibers under the load during a pressing step. Equation 20 is a mathematical expression:

$$S_b = S_{bi} + (S_h - S_{bi})(1 - e^{-P_k P}) \quad (20)$$

where

S_{bi} = fiber contact area entering nip, cm^2

S_h = maximum specific surface area of the fibers, cm^2

P = pressure, psi

P_k = pressure coefficient.

The definition of P_k conforms to the Han power law function for densification by wet pressing. It also accounts for excessive densification through several press nips. Equations 21–24 provide for its calculation:

$$P_k = -\ln(Z)/60 \quad (21)$$

$$Z = 1 - [S_{bi}/(S_h - S_{bi})]e^{[AP + BP\ln(60)]} \quad (22)$$

$$AP = 0.4 + 1.27\times10^{-4}CSF \quad (23)$$

$$BP = (3.0)10^{-3}CSF - 1.5\times10^{-4}Y \quad (24)$$

The expression for P_k is intended to account for the lower pressure and longer pressing time conditions of a handsheet mold as well as the shorter duration and higher peak pressure impulse conditions of a commercial press nip. The degree of densification correlates with the water removal in the nip. For multiple nips the contact area exiting one nip becomes the area entering the next nip. The forming blocks determine the initial unpressed fiber contact function. This relates to the fiber specific surface, S_h, and fiber conformability which depends on pulping yield given by Eq. 25:

2. Machine paper MD modulus

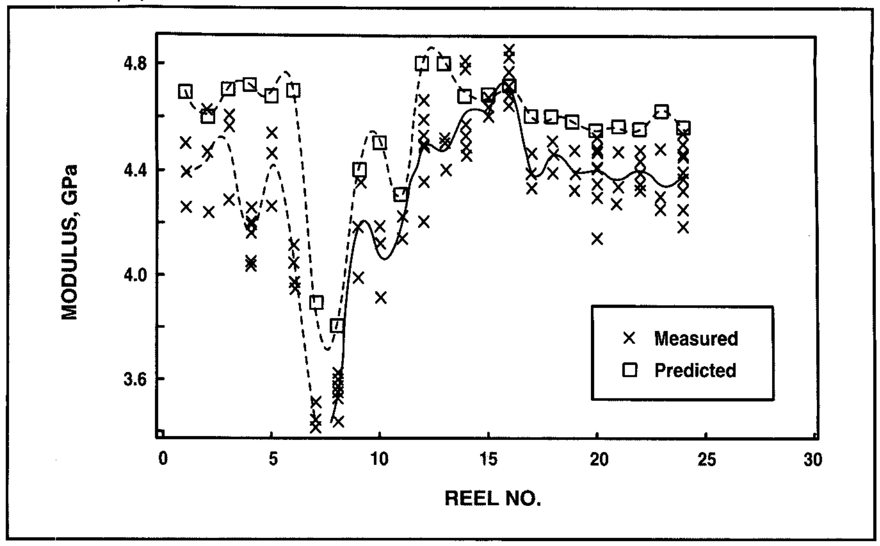

$$S_{bi} = (0.0734 - 0.000654Y)S_h \quad (25)$$

Equation 26 indicates the relationship between S_h and CSF in the fiber contact relationship:

$$S_h = 95.7 - 0.12CSF \quad (26)$$

Equations 27 and 28 provide the relationship between CSF and hydrodynamic specific surface area:

$$CSF = e^{7-0.33A} \quad (27)$$

$$A = \left[1 - \sum_{i=1}^{10} X_i \ln\left(\frac{L_i}{2.4}\right)\right]^{1/K} \quad (28)$$

where

X_i = weight fraction of fiber i

L_i = average length of fiber i, cm

K = factor accounting for differences in surface area development.

K depends upon the uniformity and extent of refining, the species, and the pulping operation as well as on external fibrillation (*5*). There are additional relationships between the fiber length distribution, surface area per fiber, and S_h which are described eleswhere. Refining influences fiber length and width distribution, CSF, and fiber stiffness factor. There also is a small influence on fiber tensile strength and modulus. These relationships depend on specific power and energy in the refining zone. Mixing brings together various types of fibers. The mixture characteristics tend to reflect the weight average composition of the various streams.

Separations in screening and cleaning in the machine system have little significant effect on the average fiber attributes entering the forming section. In dirty furnishes, however, these operations remove shives and dirt. Therefore, they improve the effective bond density, modulus, and compressive strength.

At the forming wire there is selective fines removal to the white water. This point of the operation imparts basis weight, fiber contact area, formation, and fiber orientation to the sheet. The measurement of formation efficiency relates to the coefficient of variation in mass density and ranges from 0 to 1. The formation factor is a function of forming consistency, average fiber length, I, °SR, and jet-to-wire ratio as seen in Eqs. 29 and 30:

$$F = 0.01f_l JWR \quad (29)$$

$$f_l = 119.65 - 25CO - 27.4L - 0.09(°SR) + 0.23(°SR)(L) \quad (30)$$

where

JWR = jet-to-wire ratio

3. Machine paper Concora test

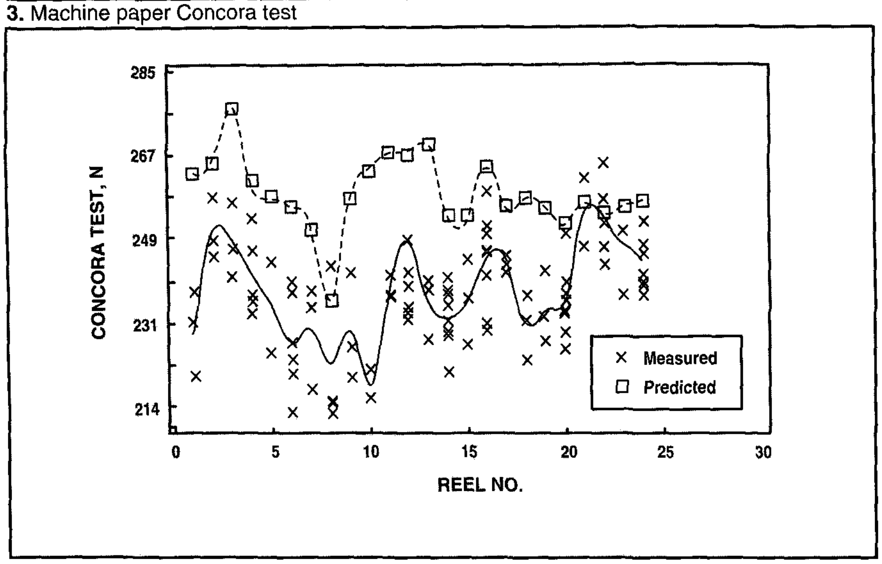

CO = forming consistency

L = average fiber length, cm.

Equation 31 provides the definition for °SR:

$$°SR = (950 - CSF)/12.5 \qquad (31)$$

The product of JWR times C equals 1 unless the conditions of Eqs. 32 and 33 occur:

$$JWR(C) = JWR/0.9;\ 0<JWR<0.9 \qquad (32)$$

$$JWR(C) = 1.1/JWR;\ JWR>1.1 \qquad (33)$$

Equation 34 defines the MD to CD tensile strength ratio:

$$R_{MD/CD} = 0.335 - 0.583WS + 0.708WS\Theta + 0.6345\Theta^2 \qquad (34)$$

where

WS = %MD wet stretched

Θ = contangent of the average fiber orientation angle.

Data analysis

We assumed that we could analyze transient process data using a steady-state simulation model with variable, i.e., transient, inputs.

We measured variance on the distribution about the mean for a total of 114 machine paper samples and 120 handsheet samples using 10 to 20 replicates per sample. The pooled test average determined the overall test variance for each machine paper or handsheet property. The pooled data for each reel interval included three CD sets and three rolls per reel. There were no measurement variances for density, basis weight, and caliper since these had only a single measurement per sample. **Table III** shows the mean, coefficient of variation (CV), correlation coefficient, and confidence band for each of the machine paper properties. The confidence band is the measurement variance percentage defined earlier. The confidence bands for each variable are twice the standard deviation divided by the mean and expressed as a percentage.

Regression of the predictions against the measurements using a single factor model with no intercept determined the correlation coefficient.

$$P_m = CP_p \qquad (35)$$

where

Pm = measured value

Pp = predicted value

C = correlation coefficient.

Thus the correlation coefficient determines the avrage correction to the predictions needed to "agree" with the measurements. All R^2 values exceeded 0.995. The high R^2 values indicated that it was possible to correct the models to agree closely with the data. The proximity of the correlation coefficient to unity indicates that the corrections are not excessive. The comparison of the difference of the correlation coefficient from unity with the corresponding confidence band in Table III also indicates that the uncorrected predictions fall within the measurement error. These statistical tests indicate that the models are generally valid for corrugating medium.

Similar conclusions arise from the handsheet data summarized in **Table IV**. Although both the measurement variance and the model error are larger for the handsheet data, the corrected models predict most of the measurement variations. With the exception of porosity the corrections are not excessive.

The zero-span tensile strength of the lightweight hand sheets varied from 6.7 km to 12 km, with a mean of 9.0 km. This indicates that the assumed average fiber tensile strength attribute of 9.5 km from Table I was reasonable.

Process variable effect on machine paper properties

The simultaneous variation in several process conditions caused difficulties in obtaining meaningful machine or handsheet property profiles vs. reel number. Therefore, we determined the effects of the process variables by comparing the mean property values and by statistical regression.

Figures 1–3 show the profiles for caliper, MD modulus, and Concora test plotted against reel number. Each measured value indicates the average measurement of a roll or set for each reel. Except for the obvious effect of calender stack unloading for reels 7 and 8, the effects of other variables are difficult to discern readily.

Machine speed and calender load

Table V shows that neither machine speed nor calender load affected the mean compressive or tensile strength properties greater than the measurement variance. Calender loading did, however, significantly change density, caliper, and elastic moduli. Increased density provided increased modulus, decreased caliper, and unchanged specific modulus. The lack of sensitivity of a specific modulus resulted in no response in compressive properties.

One might expect from the models that the calender stack loading could possibly affect the MD-to-CD ratio through stretch or stress relief. The measured properties did not support this conclusion, however.

The sheet property data correlated weakly with the trial variables, indicating that the properties were only somewhat dependent on these process variables. MD tensile strength correlated with machine speed (33%), calender loading (10%), and sheet density (5%). Burst index correlated with the product of MD and CD tensile strength (60%) as expected from the property models. Elastic moduli correlated with sheet density (50%). CD ring crush was weakly dependent on machine speed (6%), and Concora test showed a weak (10%) dependence on calender loading. Sheet density was sensitive to calender loading (40%) and less sensitive to CSF and OCC content. These percentages derive from the sum of squared error for each term. Surprisingly, neither the statistical analysis nor visual inspection of the data showed any sensitivity to refiner power or press load. Other statistical comparisons indicated that the effects of machine speed and calender load also were within measurement error.

V. Effect of calender load and machine speed

Property	Calender		Machine speed, m/s	
	On	Off	7.11	9.65
MD Modulus, GPa	4.40	3.52	4.39	4.30
CD Modulus, GPa	1.88	1.46	1.90	1.82
MD/CD Modulus ratio	2.35	2.35	2.35	2.35
Tensile strength, km	5.81	5.97	5.72	6.08
Burst index	2.90	2.88	2.79	2.96
Density, g/cm^3	0.60	0.52	0.595	0.59
Caliper, mm	0.209	0.245	0.206	0.214
Concora test, N	223.4	239.8	242.8	236.4
CD STFI, kN/m	2.54	2.56	2.56	2.50
CD ring crush	0.97	0.77	0.92	1.02

OCC content

Although OCC content varied from 18% to 36%, there was only a relatively minor effect on compressive properties. The MAPPS models show that the OCC fiber attributes are similar to those of the semichemical fibers. Therefore, the mixture attributes did not change greatly with increasing OCC. Visual inspection of the data indicated that tensile strength and burst were highest near the peak in OCC. The freeness of the mixture did decrease with increasing OCC content. This gave increased sheet density, reduced caliper, and increased modulus. The specific modulus and compressive strength did not change significantly, however.

MD modulus increased about 0.9 GPa (approximately 30%). CD modulus increased by 0.42 GPa (approximately 25%). The CD ring crush increased by 0.196 (25%). This is comparable to the measurement standard deviation and is judged to be insignificant change. Concora test changed less than the measurement standard deviation. It was not significant at 90% confidence.

The model sensitivity analysis and visual inspection of the data indicated that increasing OCC content improved tensile strength, burst, and ring crush mainly through decreased CSF and improved bonding. The highest tensile strength and burst values occurred during the period just after the peak in OCC content from 35% down to 30%. Tickler discharge CSF also was relatively high with a value of 450 mL. Primary refiner power was 0.19 mJ/kg. Third-nip press load also was at its high value of 113.83 Kn/m. A sensitivity analysis with the model showed that the tensile strength and compressive properties increased slightly with increasing OCC content, primarily due to its decreasing freeness. The increase in burst index and breaking length is about 10% for the maximum variation in OCC content in the test.

Refining and wet pressing

Increased refining power tended to decrease tensile and burst, while sheet density, porosity, and modulus increased. A high refining power decreased tensile strength and burst through decreased fiber tensile strength. Contrary to conventional wisdom, the high refining power also increased sidedness and decreased average bond area. Press had very little effect. Refining and pressing had indirect effects, mainly in sheet water removal and steam consumption in the dryer.

Conclusions

Based on the two validation criteria and estimates of measurement error, the model system in our study was valid for corrugating medium. Calculated correction factors are necessary for some of the property predictions. While the measurements did not correlate with the test variables by standard methods, they correlated strongly with model predictions with relatively small corrections. Sensitivity analysis with the validated models showed that OCC content improved tensile strength but had little effect on compressive strength. This is contrary to most expectations.

Calender load and machine speed had only a minor effect on most properties. Statistical analysis showed that both press load and refining power had no effect on properties under these conditions. Sensitivity analysis showed that refining may have negatively affected tensile strength properties. These were also surprising findings. There was some evidence that machine speed affected MD tensile strength. Tensile strength and modulus ratios also were insensitive to test variables. There was evidence of transient effects based on the handsheet CSF and machine paper data, but these effects were inseparable from the overall variations in the data. Future simulations may clarify the roll of transient effects.

Literature cited

1. Jones, G. L., Pulp Paper Can. 89(6): T213(1987).
2. Jones, G. L., Tappi J. 72(10): 189(1989).
3. Jones, G. L. and Nguyen, X. N., Tappi J. 73(7): 160(1990).
4. Jones, G. L., Tappi J. 73(11): 113(1990).
5. Jones, G. L., Pulp Paper Can. 91(2): T81(1989).

The author thanks the member companies of the Institute of Paper Science and Technology. He especially thanks the personnel at MacMillan Bloedel, Pinehill, AL, for their support and assistance with this work.

Received for review Nov. 3, 1992.

Accepted Jan. 17, 1993.

Presented at the TAPPI 1992 Papermakers Conference

Letters, continued from page 14

additional 800,000 tons at a 70% yield, 10% substitution level, 10% filler content, and 5% moisture would equate to over 6.4 million scale weight tons per year. If 50% of that production is sourced from the post-consumer stream, then more than 3 million additional tons per year could be so labeled.

I stand by my view about the "anti-business" tone of the book, particularly as related to clearcutting. Our forests are a resource in our stewardship. Clearcutting is not appropriate in New York State on a tree farm. But the same is not true in the Northwest, where we are talking of a different species. Why would responsible stewards devalue their own resource?

My acknowledged bias as a representative of Weyerhaeuser, comes not from the basis that it is one of the "largest fully integrated virgin paper companies", but rather from the fact that Weyerhaeuser is a leader in recycling efforts. Our Recycling Division collects over 2 million tons of paper per year for our own operations, as well as other paper companies.

At the end of the 1980s, we were recycling about 1100 tons per day, but we didn't talk about it. In 1991, we brought on line a 600 tpd newsprint deinking mill at our Longview complex. In 1992, a 500 tpd expansion at mill in Valliant, OK. In a few months, a 500 tpd greenfield OCC operation will start at Springfield, OR. In 1994, we will add a new 600 tpd line at Plymouth, NC, and in 1995, expand the existing system to 600 tpd. Plus, we are in the planning stages for a 100% recycled mill in the Midwest. Our fine paper machines use purchased recycled fiber from third party market pulp mills. When it makes economic sense, we'll make our own.

Recycling of secondary fiber is as interesting today as it was when I first became involved nearly 25 years ago. Then, we didn't talk about it--we just did it.

—Richard Spangenberg
Director, Recycling Research
Weyerhaeuser Paper Company